Geomechanics and Engineering, *Vol. 41, No. 2 (2025) 243-254*
https://doi.org/10.12989/gae.2025.41.2.243

Effect of standoff distance and abrasive particle size on abrasive waterjet drilling of hard rock: A numerical study

Hyun-Joong Hwang[1a], Yohan Cha[2b], Joohyun Park[3c] and Gye-Chun Cho*[3]

[1]*Applied Science Research Institute, Korea Advanced Institute of Science and Technology (KAIST), 291 Daehak-ro, Yuseong-gu, Daejeon 34141, Republic of Korea*
[2]*Disposal Performance Demonstration R&D Division, Korea Atomic Energy Research Institute (KAERI), 111 Daedeok-daero, 989beon-gil, Yuseong-gu, Daejeon 34057, Republic of Korea*
[3]*Department of Civil and Environmental Engineering, Korea Advanced Institute of Science and Technology (KAIST), 291 Daehak-ro, Yuseong-gu, Daejeon 34141, Republic of Korea*

(*Received December 7, 2024, Revised March 14, 2025, Accepted April 13, 2025*)

Abstract. Abrasive waterjet technology offers high efficiency in drilling high-strength materials such as rock and concrete, and is utilized in various fields such as precision machining, geotechnical engineering and mining engineering. Previous studies have analyzed the jet flow characteristics in air through experimental, analytical, and numerical approaches; however, they were primarily limited to short standoff distances and single-sized abrasive particles, limiting their application to large-scale geotechnical and mining engineering sites. To overcome these limitations, this study performed a numerical analysis considering various standoff distances and abrasive particle sizes. This study observed jet flow characteristics in the axial and radial directions and evaluated the abrasive velocity and kinetic energy. In addition, the critical energy for rock drilling was derived to be approximately 0.36 J from the simulation results based on the minimum critical pressure for hard rock excavation. Based on this value, an effective jet diameter that considers the number of abrasive particles was proposed for various standoff distances and abrasive particle sizes. The abrasive particle size significantly affected the effective jet diameter when the standoff distance was greater than 100 mm. This study aims to expand the applicability of abrasive waterjet technology in geotechnical and mining fields and provide essential guidelines for optimizing an efficient system design and abrasive selection strategy under various field conditions.

Keywords: abrasive waterjet; effective jet diameter; jet flow characteristics; numerical method; rock drilling

1. Introduction

Underground space development is becoming vital for solving challenges such as space shortages in urban areas owing to urbanization and infrastructure expansion. The tunnel boring machine (TBM) method is primarily used for rock excavation (Gong *et al.* 2016, Liu *et al.* 2016). The TBM method has high stability because it can minimize the vibration and impact on surrounding underground structures; however, there are problems such as low efficiency in hard and heterogeneous rocks and limitations in application in narrow environments. Recently, attempts have been made to improve excavation efficiency by optimizing equipment operation according to ground conditions by combining machine-learning techniques (Samadi *et al.* 2023, Hwang *et al.* 2024a, Samadi *et al.* 2024). However, excavating hard rock still causes serious wear on the disc cutter, which increases maintenance costs and demands high thrust forces (She *et al.* 2023, Lee *et al.* 2023). Abrasive waterjet (AWJ) technology has attracted considerable attention for overcoming these limitations. It operates in a non-contact manner to minimize mechanical wear and provides high energy density, even with small-scale equipment; thus, it can be effectively applied even in narrow underground environments (Lu *et al.* 2013, Liu *et al.* 2017, Zhang *et al.* 2020, Li *et al.* 2022). In addition, AWJ technology is a highly efficient method that can cut or drill various ductile (e.g., stainless steel and titanium alloys) and brittle (e.g., concrete and hard rock) materials using high-pressure water and abrasives and is particularly effective in drilling high-strength materials such as rocks (Summers 2003, Horszczaruk 2009, Momber 2011).

The drilling width of the rock is a critical indicator for the practical application of AWJ in rock drilling. For an effective rock drilling performance, the nozzle of AWJ must be inserted into the drilled hole before proceeding with drilling. Therefore, it is necessary to secure the width of the drilled hole for inserting the AWJ nozzle. The drilling width of the rock is primarily affected by the jet diameter when the rock is impacted by the jet. Therefore, the drilling width should be accurately predicted through an effective understanding of the jet diameter to reflect the jet dispersion characteristics. There is limited research on the drilling width of rocks, though some researchers have experimentally evaluated the cutting kerf width of rocks using AWJ (Hashish 1991, Karakurt *et al.* 2012, Momber

*Corresponding author, Professor
E-mail: gyechun@kaist.edu
[a]Postdoctoral Researcher
[b]Senior Researcher
[c]Ph.D. Candidate

ISSN: 2005-307X (Print), 2092-6219 (Online)

and Kovacevic 2012, Karakurt *et al.* 2014). Kerf width has been evaluated to be affected by various parameters, such as water pump pressure, abrasive flow rate, standoff distance, and abrasive particle size. Previous studies have been conducted experimentally under conditions with limited abrasive particle sizes (i.e., 80 and 120 mesh) and short standoff distances (i.e., less than 10 mm) at the laboratory scale. Therefore, there is a limitation in considering the jet dispersion characteristics in air, limiting the accurate determination of jet diameter. Moreover, it is challenging to apply these results to actual field environments that require scale expansion, such as the geotechnical or mining fields. This is because when the standoff distance is small, collisions may occur between the waterjet nozzle and the irregular target rock surface existing in the field; hence, a relatively long standoff distance (e.g., greater than 100 mm) is required (Oh and Cho 2016).

Previous researchers have approached the jet flow characteristics in the air through various ways: experimentally, analytically, and numerically. Yanaida and Ohashi (1974) experimentally observed the jet flow characteristics and developed a mathematical model based on momentum conservation as an analytical approach. They classified the jet structure into three zones: core, transitional, and main, and defined the core and transitional zones together as the initial zone. However, their model was developed at a low water pump pressure of up to 50 MPa, which limits its application to hard rocks. Isobe *et al.* (1988) and Hou *et al.* (2010) experimentally measured jet velocity using the impact crater counting method and impact force measurements, respectively. However, these methods cannot observe the velocities of water and abrasive particles separately. Therefore, they have limitations in observing the kinetic energy of abrasive particles, which plays a substantial role in rock material removal. Zeleňák *et al.* (2016) used particle image velocimetry (PIV) technique combined with laser induced fluorescent (LIF) method to distinguish and measure abrasive particle velocity experimentally. However, these methods are limited by the high cost of the equipment and the potential variability in accuracy depending on the performance of the equipment. Liu *et al.* (2003) and Liu *et al.* (2004) numerically observed the jet flow characteristics using a computational fluid dynamics (CFD) model. They performed simulations under steady state, turbulent, and three-phase flow conditions and observed the jet flow by applying an axisymmetric flow. However, they input a specific peak velocity (e.g., 600–900 and 950 m/s) as the inlet boundary condition of the jet flow without considering the abrasive particle size, and the investigation was conducted at short standoff distances (e.g., 10 and 50 mm), which limited their application to rock drilling sites. Wang and Wang (2010) developed an AWJ flow model based on the fundamental laws of conservation as an analytical approach and numerically analyzed the jet flow. However, their results were limited to a short range of standoff distances (e.g., 1–10 mm) for uniformly sized abrasive particles. Thus, their application in geotechnical or mining fields requires a relatively long range of standoff distances (e.g., greater than 100 mm).

Previous studies observed jet flow characteristics through various experimental, analytical, and numerical approaches and provided critical insights into jet dispersion and energy transfer mechanisms. Although these studies

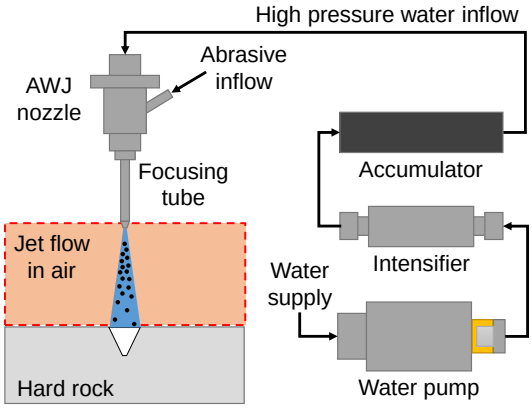

Fig. 1 Schematic of the AWJ drilling system

have contributed considerably to the understanding of the basic principles of AWJ technology, they have several limitations when applied to geotechnical and mining fields. First, previous studies primarily analyzed relatively short standoff distances, which failed to sufficiently reflect the larger standoff distance conditions required in the field. Numerical analysis in prior works typically assumed an idealized uniform velocity distribution at the focusing tube nozzle exit, which had limitations in completely capturing the real-world jet dispersion characteristics. In addition, assuming a uniform abrasive particle size or restricting the analysis to a limited range made it challenging to accurately assess the influence of varying particle sizes on jet flow and dispersion characteristics in air.

Hence, this study aims to systematically analyze the jet flow characteristics of AWJ in air using a numerical approach that incorporates a wider range of standoff distances and various abrasive particle sizes, thereby extending the scope of previous studies. Unlike conventional numerical analyses that assume an idealized uniform velocity at the focusing tube nozzle exit, this study applies a realistic velocity distribution obtained from a validated numerical model, ensuring a more accurate representation of jet dispersion characteristics. Furthermore, this study proposes to derive the effective jet diameter based on key variables (i.e., standoff distance and abrasive particle size) to more precisely evaluate the applicability of AWJ at the field scale. The findings will provide fundamental data for AWJ system design and abrasive selection strategies, as well as insights into optimizing AWJ performance in geotechnical and mining applications, such as rock drilling.

2. Theoretical background

In rock drilling using AWJs, abrasives play a critical role in material removal, and it is vital to maximize the kinetic energy of the abrasives to achieve effective performance (Momber 2004, Nambiath et al. 2007). The kinetic energy of the abrasive is the primary energy source of the AWJ method, and the abrasive undergoes several acceleration and deceleration processes from the waterjet system into the air until it drills through the rock (Fig. 1).

First, the high-pressure water generated in the water pump system passes through a small-diameter orifice and is converted into high-speed water, gains energy, and moves into the mixing chamber. The abrasive was mixed with water in a mixing chamber and transferred to a focusing tube. In this process, the abrasive receives the momentum of water and accelerates to gain energy. The water-abrasive mixture passing through the focusing tube was aligned in a linear flow, had a terminal velocity, and was jetted into air in the form of a jet (Momber and Kovacevic 1995, Roth *et al.* 2005). The jet sprayed into the air disperses and loses energy owing to air resistance. Consequently, the range and energy of the jet at the point of impact on the rock material directly affect rock drilling.

To define the jet range and energy when the jet first strikes the rock to remove the rock material, it is necessary to calculate the total number of abrasive particles ($N_{a,t}$) injected into the AWJ system. This is because the number of abrasive particles differs at each radial position owing to the dispersion of the jet and abrasive. Assuming that the abrasive particles are spherical, the single-particle abrasive mass (m_a) is defined by Eq. (1), and the total number of injected abrasive particles ($N_{a,t}$) was calculated using Eq. (2).

$$m_a = \frac{\pi}{6} \cdot {D_a}^3 \cdot \rho_a \tag{1}$$

$$N_{a,t} = \frac{\dot{m}_a}{m_a} \cdot t \tag{2}$$

Here, D_a is the abrasive particle diameter, ρ_a is the abrasive particle density, $\dot{m}_a$ is the abrasive flow rate, and t is the exposure time.

The kinetic energy of a single abrasive particle (E_a) was defined using Eq. (1) as

$$E_a = \frac{1}{2} \cdot m_a \cdot {v_a}^2, \tag{3}$$

where v_a is the abrasive particle velocity.

In addition, the abrasive particles in the air are densely concentrated at the center of the jet, and the number of particles decreases in the radial direction (Balz and Heiniger 2011). Therefore, assuming that the abrasive particle distribution for the radial position (r) follows a Gaussian distribution, the probability density function of the abrasive particle distribution ($f(r)$) is expressed as follows

$$f(r) = \frac{1}{\sqrt{2\pi}\sigma} e^{-\frac{r^2}{2\sigma^2}}, \tag{4}$$

where r is the radial position, and σ is the standard deviation.

The standard deviation (σ) was set to thrice the standard deviation of the radial position range so that 99.7% of the abrasive particles exist in the probability density function of abrasive particle distribution ($f(r)$). In addition, to determine the boundary point, the point at which the abrasive velocity was less than 1 m/s was set as the radial boundary position (r_b). The standard deviation (σ) is defined as follows

$$\sigma = \frac{r_b}{3}. \tag{5}$$

From $f(r)$ of Eqs. (2) and (4), the number of abrasive particles at the radial position ($N_a(r)$) can be defined as follows

$$N_a(r) = N_{a,t} \cdot f(r) \cdot \Delta r, \tag{6}$$

where Δr is the radial position interval.

Moreover, from Eqs. (3) and (6), the total abrasive kinetic energy at the radial position ($E_{a,t}(r)$) is calculated as follows

$$E_{a,t}(r) = E_a \cdot N_a(r). \tag{7}$$

The critical energy for rock drilling (E_c) can be determined through numerical analysis, utilizing the minimum critical pressure derived from experiments in previous studies. The critical jet radius (R_c) is defined as the length to the radial position corresponding to the determined critical energy for rock drilling (E_c) and can be calculated by the following relationship

$$E_{a,t}(R_c) = E_a \cdot N(R_c) = E_c. \tag{8}$$

Finally, the effective jet diameter (D_{jet}) at the moment of impact during rock drilling is defined as follows

$$D_{jet} = 2 \cdot R_c. \tag{9}$$

3. Numerical method

3.1 Numerical setup

Numerical simulations were performed using ANSYS Fluent, a CFD software based on the finite-volume method (Fluent ANSYS 2023). ANSYS Fluent can analyze multiphase flows and various types of geometries, such as 2D and 3D. Therefore, ANSYS Fluent is suitable for modeling and analyzing AWJs that require complicated analyses involving fluid and solid phases. In this study, ANSYS Fluent was used to analyze the behavior of an AWJ in air.

The multiphase flow of an AWJ system is classified into continuous phases, such as air or water, and discrete phases, such as abrasive particles. In this simulation, the volume of fluid model, which is a Eulerian approach typically used in multiphase analysis, was applied to simulate the continuous phase (Liu *et al.* 2004, Zou *et al.* 2024). A standard k-epsilon model was applied to consider the turbulent flow and viscosity of the continuous phase (Launder and Spalding 1983). In addition, a discrete phase model, which is a Lagrangian approach, was applied to simulate the solid abrasive particles, and an analysis was performed (Jafar *et al*. 2015, Lv *et al*. 2018). In addition, the discrete random walk model was applied to accurately calculate the behavior of abrasive particles in a turbulent flow in the fluid (Hwang *et al.* 2024b).

In this simulation, to observe the movement and velocity of the abrasive sprayed from the AWJ system in air, the geometry formed an air zone together with a portion of the tip of the focusing tube. To consider the 3D behavior of the abrasive in air, a 2D axisymmetric space was applied based on the central axis of the jet (Fig. 2). The inlet represents the tip of the focusing tube of the AWJ system and provides flow just before the jet is sprayed into the air. Assuming that a jet comprising a mixture of water and abrasive becomes a fully developed flow at the tip of the focusing tube, the velocity distribution of the

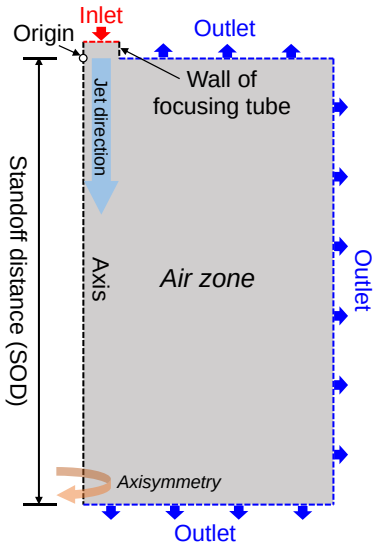

Fig. 2 Geometry and boundary condition positions of the simulation model

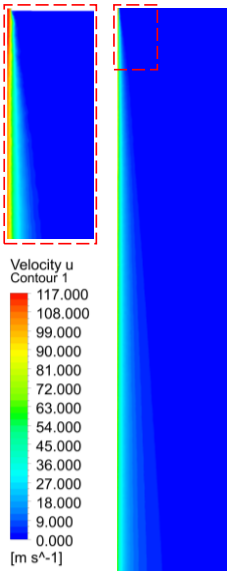

Fig. 3 Axial abrasive velocity contour of the numerical simulation

jet (v_{jet}) follows the 1/7th power law (Streeter and We 1998, Alberdi *et al.* 2010, Nagaraja and Devadula 2023). The velocity distribution of the jet (v_{jet}) is expressed as follows

$$v_{jet} = v_{max}\left(1 - \frac{2r}{D_f}\right)^{1/7}, \tag{10}$$

where v_{max} is the maximum velocity of the jet generated at the end of the focusing tube along the central axis, r is the radial position, and D_f is the diameter of the focusing tube. v_{max} was applied using the resulting value derived from the AWJ 3D model of Hwang *et al.* (2024b) in a previous study. The radial position (r) follows the range of $-\frac{D_f}{2} \le r \le \frac{D_f}{2}$.

Wall applied the restitution coefficient (μ) to consider the collision between the wall of the focusing tube and the abrasive

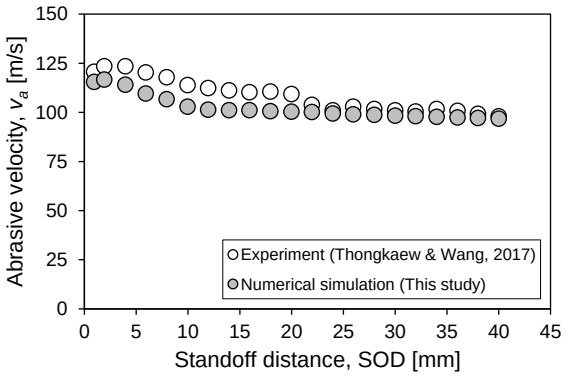

Fig. 4 Comparison of abrasive particle velocity for validating the numerical model

particles (Forder *et al.* 1998). In this study, the abrasive particles were modeled as perfectly spherical to simplify computational modeling and ensure consistency with previous numerical studies. This assumption allows for a more systematic analysis of abrasive particle-wall interactions while reducing computational complexity. The restitution coefficient (μ) is defined as a polynomial for the particle incidence angle and is expressed as follows

$$\mu_{\perp} = 0.988 - 0.78\theta + 0.19\theta^2 - 0.024\theta^3 + 0.027\theta^4,$$
$$\mu_{/\!/} = 1 - 0.78\theta + 0.84\theta^2 - 0.21\theta^3 + 0.028\theta^4 - 0.022\theta^5, \tag{11}$$

where $\mu_{\perp}$ is the restitution coefficient for the normal direction, $\mu_{/\!/}$ is the restitution coefficient for the tangential direction, and θ is the particle incidence angle.

The outlet was set to an atmospheric pressure of 101.325 kPa to simulate an air zone in which the jet could disperse. The convergence of the simulation model was achieved when the residuals for all physical quantities were less than 0.0001.

3.2 Model validation

In this study, the numerical model was validated and compared with the experimental results obtained by Thongkaew and Wang (2017). To achieve this, the simulation conditions were set to match those of the experimental setup as closely as possible, ensuring a direct and meaningful comparison. The validation process focuses on assessing whether the numerical model can accurately capture the key flow characteristics of the abrasive waterjet, particularly in terms of abrasive particle velocity. Thongkaew and Wang (2017) experimentally observed the abrasive particle velocity in air using PIV and LIF techniques. Their test used an AWJ system with the following conditions: orifice diameter of 0.254 mm, focusing tube diameter of 0.76 mm, focusing tube length of 76.2 mm, water pump pressure of 10 MPa, abrasive flow rate of 0.3 g/s, abrasive particle size of 0.18 mm, and abrasive particle density of 4100 kg/m^3. They observed the abrasive particle velocity for a standoff distance of 40 mm from the end of the focusing tube. Therefore, in this study, a numerical analysis was performed by modeling the

Table 1 Simulation cases and details

Parameter [Unit]	Value				
Water pump pressure [MPa]	320				
Water flow rate [ml/s]	50.01				
Abrasive flow rate [g/s]	5				
Orifice diameter [mm]	0.33				
Focusing tube diameter [mm]	1.02				
Focusing tube length [mm]	76.2				
Abrasive particle density [kg/m^3]	3790				
Abrasive particle size [mm]	0.07	0.09	0.18	0.25	0.40
Standoff distance [mm]	10	10	10	10	10
	50	50	50	50	50
	100	100	100	100	100
	150	150	150	150	150
	200	200	200	200	200
	250	250	250	250	250

conditions of an AWJ system identical to the experimental one. The results of the numerical analysis are shown in Fig. 3, and the maximum abrasive particle velocity was observed at the center axis of the jet for each standoff distance.

The results of the comparison between the experimental values from the previous study and the numerical simulation values from the present study are shown in Fig. 4. Although some discrepancies in velocity values were observed at low SOD, primarily due to air turbulence effects and boundary layer effects near the focusing tube nozzle exit, these variations had a limited impact on the overall accuracy of the model. At very short standoff distances, the interaction between the high-speed jet and the surrounding air induces turbulence, leading to velocity fluctuations. Additionally, the velocity profile near the focusing tube nozzle exit is not fully developed, which can contribute to measurement deviations. Despite these localized discrepancies, the average error across all cases was approximately 4.98 %, indicating that the numerical model effectively captures the overall jet flow characteristics. Therefore, the proposed numerical approach is considered sufficiently validated for analyzing the jet flow behavior under various standoff distance conditions.

3.3 Simulation cases

To observe the effects of the standoff distance and abrasive particle size on the effective jet diameter and impact energy when drilling rocks using an AWJ, different abrasive particle sizes and standoff distances were used in the numerical simulation. Unlike the validation study, where parameters were fixed to replicate experimental conditions, this section explores a broader range of simulation cases to analyze trends and dependencies that may not have been covered in the experimental setup. The objective of this study is to provide a comprehensive understanding of how jet behavior changes under different operating conditions, which is critical for optimizing AWJ drilling performance in real-world applications. Therefore, the inlet was defined as the tip of the focusing tube, requiring input values for simulation in this study. For this purpose, the Hwang *et al.* (2024b) model for numerical analysis of the AWJ system was utilized to determine the velocity and volume fraction at the tip of the focusing tube for various abrasive particle sizes. These results were applied to this simulation. The AWJ system parameters, simulation cases, and their details are listed in Table 1.

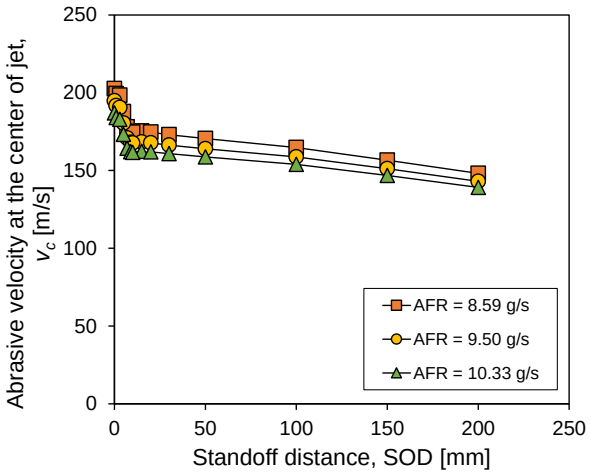

Fig. 5 Abrasive velocity at the center of jet under critical pressure conditions of 90 MPa

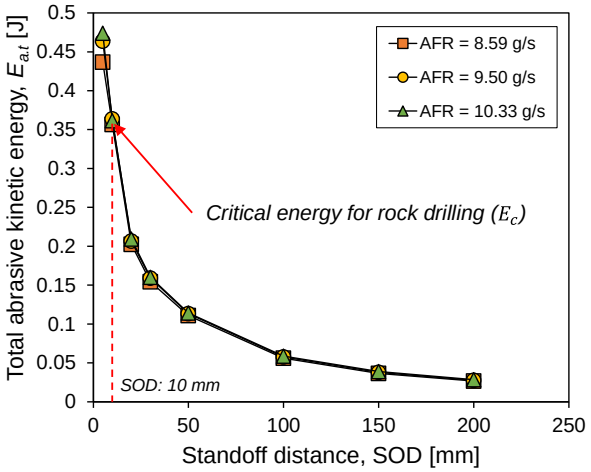

Fig. 6 Critical energy of the abrasive particle for hard rock drilling

4. Results and discussion

4.1 Critical energy of the abrasive particle for rock drilling

Previous studies have shown that a minimum critical pressure is required to excavate hard rock, which is a brittle material such as granite (Evans *et al.* 1978, Oh and Cho 2014, Cha *et al.* 2021). Oh and Cho (2014) applied three water pump pressures (157, 235, and 314 MPa), three

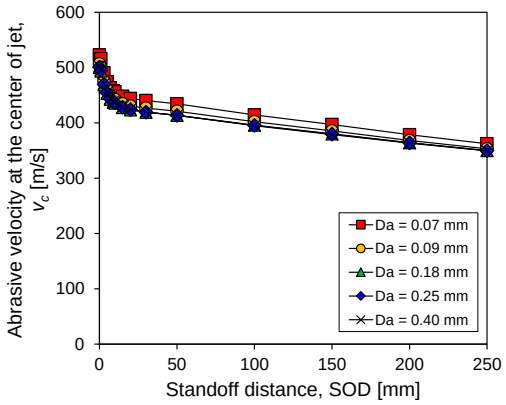

(a) Abrasive particle velocity

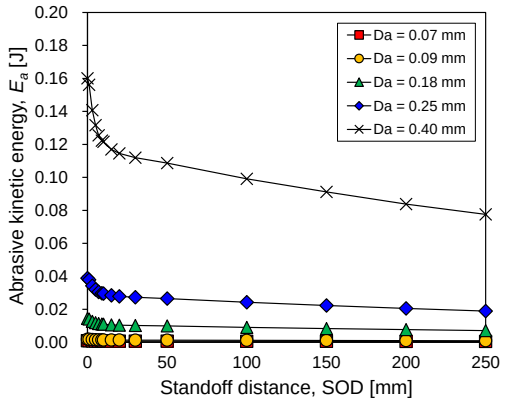

(b) Kinetic energy of abrasive particles

Fig. 7 Axial velocity and kinetic energy of the abrasive article at the center of the jet

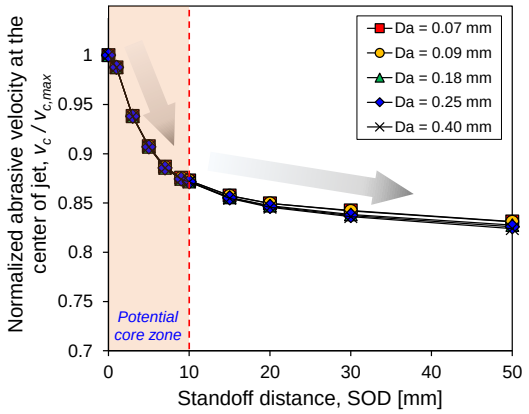

Fig. 8 Jet potential core zone along the axial direction

Table 2 Simulation cases and details of critical energy determination

Parameter [Unit]	Value		
Water pump pressure [MPa]	90		
Water flow rate [ml/s]	15.39		
Orifice diameter [mm]	0.254		
Focusing tube diameter [mm]	0.76		
Focusing tube length [mm]	76.2		
Abrasive particle density [kg/m^3]	3790		
Abrasive particle size [mm]	0.18		
Abrasive flow rate [g/s]	8.59	9.50	10.33
Standoff distance [mm]	0–200	0–200	0–200

corresponding abrasive flow rates (8.59, 9.64, and 10.33 g/s), and three traverse speeds (1.9, 8.4, and 14.1 mm/s) to conduct rock cutting experiments using an AWJ at a standoff distance of 10 mm. They observed that a minimum critical pressure of 70–90 MPa was required for rock excavation regardless of the traverse speed. In this study, a numerical analysis was performed by modeling an AWJ system identical to the experimental conditions of Oh and Cho (2014) to determine the critical energy for rock drilling. The geometry and boundary conditions used in the numerical analysis are summarized in Table 2. To determine the critical energy conservatively, the water pump pressure was set to 90 MPa, which is the largest value in the minimum critical pressure range.

Fig. 5 shows the results of the abrasive velocity at the center of the jet (v_c) with respect to the standoff distance. As the standoff distance increased, the abrasive velocity decreased owing to air resistance. In addition, the abrasive velocity formed at the same pressure of 90 MPa (i.e., the minimum critical pressure) changed with the abrasive flow rate. This is because the number of abrasive particles injected increases with the abrasive flow rate; thus, relatively more particles share and receive the limited water energy. Eventually, the number of abrasive particles significantly influences the determination of the abrasive kinetic energy, which requires deep consideration. In addition, the number of abrasive particles is affected by the abrasive flow rate and the size and density of the abrasive particles; therefore, a complex understanding of the abrasive characteristics is essential (Eqs. (1) and (2)).

Fig. 6 shows the total kinetic energy of the abrasive particles ($E_{a,t}$) according to the standoff distance at a water pump pressure of 90 MPa. This result was calculated by comprehensively considering the maximum abrasive velocity and number of abrasive particles at the central axis of the jet, as shown in Fig. 5. In Fig. 5, the kinetic energy of the single abrasive particles generated according to the abrasive flow rate changes. However, when the number of abrasive particles is considered together, the energy values are similar regardless of the abrasive flow rate, as shown in Fig. 6. These values represent the energy received by the rock based on the standoff distance. According to Oh and Cho (2014), the total abrasive kinetic energy when the standoff distance was 10 mm was the maximum kinetic energy received by the rock at the central axis of the jet. Therefore, the critical energy for rock drilling (E_c) can be considered the total abrasive kinetic energy under these conditions. Consequently, through this numerical analysis, the critical energy for rock drilling (E_c) was derived as approximately 0.36 J.

4.2 Jet characteristics in the air

4.2.1 Axial characteristics of the jet

The jet characteristics in the air were analyzed by

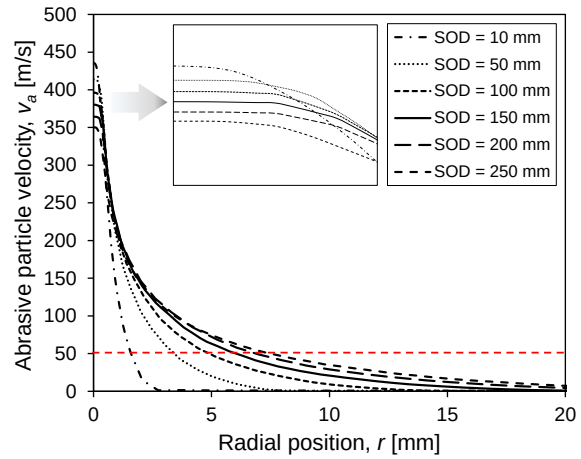

(a) Abrasive particle velocity

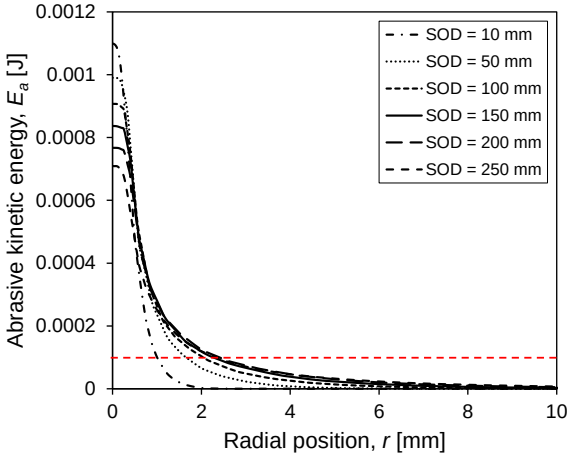

(b) Kinetic energy of abrasive particles

Fig. 9 Effect of standoff distance on the jet dispersion in air (abrasive particle size of 0.18 mm)

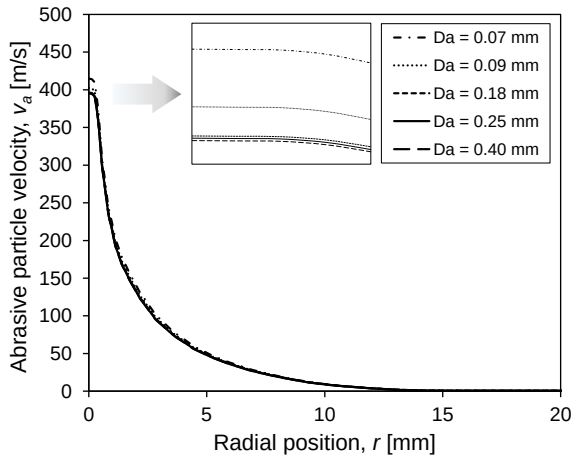

(a) Abrasive particle velocity

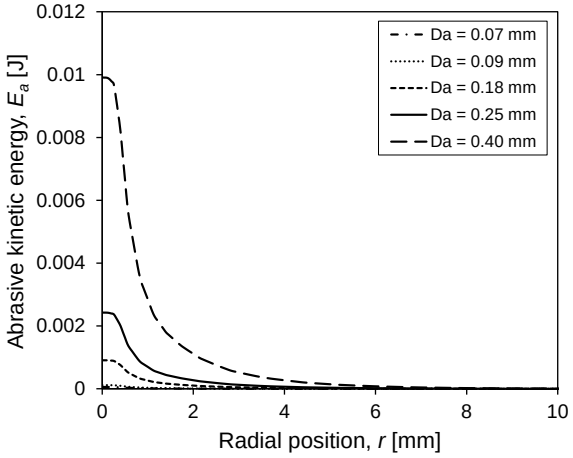

(b) Kinetic energy of abrasive particles

Fig. 10 Effect of abrasive particle size on the jet dispersion in air (standoff distance of 100 mm)

classifying them into axial and radial directions. The jet characteristics in the axial direction are shown in Fig. 7. It was confirmed that the abrasive velocity decreased owing to air resistance as the standoff distance increased for all abrasive particle sizes (Fig. 7(a)). In addition, the abrasive velocity decreased as the abrasive particle size increased under the same standoff distance. This is because the analysis was performed under the same water pump pressure (320 MPa) conditions, and the mass of the abrasive particle increased with the abrasive particle size; thus, the cceleration efficiency by water decreased. However, because the abrasive kinetic energy (E_a) considers both the mass and velocity of the particle, its trend differs from that of abrasive velocity.

Fig. 7(b) shows the effects of the standoff distance and abrasive particle size on the abrasive kinetic energy. The kinetic energy of the abrasives was calculated using Eq. (3). Similar to the abrasive velocity, the abrasive kinetic energy decreases as the standoff distance increases. However, in terms of the abrasive particle size, a relatively larger abrasive kinetic energy was generated as the size increased. Therefore, the abrasive kinetic energy is more dependent on the abrasive particle size than on the abrasive velocity. In addition, when drilling rocks using an AWJ, the drilling depth is expected to increase as the abrasive particle size increases and the standoff distance decreases.

The results obtained when the abrasive velocity was normalized to the maximum abrasive velocity at SOD = 0 mm (i.e., the tip of the focusing tube) are shown in Fig. 8. The trend of the abrasive velocity according to the standoff distance was similar for all the abrasive particle sizes. However, the rate of velocity decrease exhibited two distinct phases depending on the 10 mm threshold.

Within the first 10 mm of standoff distance, the abrasive velocity decreased significantly by approximately 13%, indicating a rapid energy dissipation phase as the jet transitioned from the high-energy potential core zone to the fully developed jet dispersion zone. This sharp reduction is attributed to the strong interaction between the jet and the surrounding air, causing increased turbulence and momentum loss.

For standoff distances greater than 10 mm, the velocity decrease became more gradual, suggesting that the primary energy dissipation had already occurred within the potential core zone, and further velocity loss was relatively minor. This behavior highlights that the effective jet energy is best

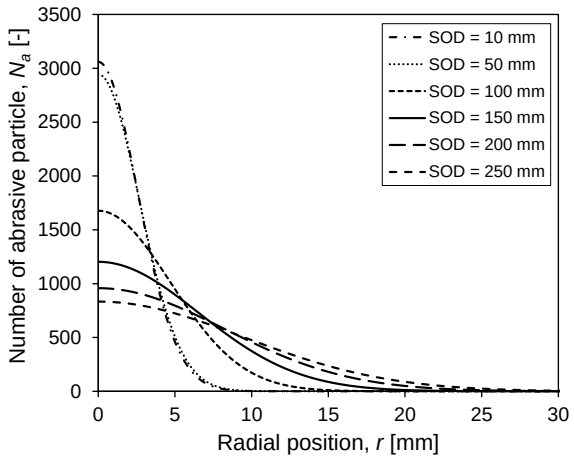

(a) Number of abrasive particles

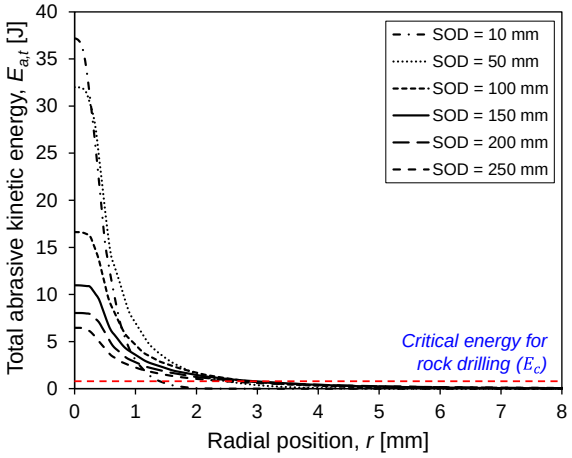

(b) Total kinetic energy of abrasive particles

Fig. 11 Effect of the standoff distance on the number and total kinetic energy of abrasive particles (abrasive particle size of 0.40 mm)

utilized within the potential core zone, reinforcing the importance of striking the jet onto the target material within this range for optimal performance in terms of drilling depth.

To clarify this transition, the potential core zone is identified as the region within SOD ≤ 10 mm, where the jet retains the highest velocity and impact energy. This observation provides critical insights into optimizing AWJ operational parameters, particularly standoff distance selection, to maximize cutting and drilling efficiency.

4.2.2 Radial characteristics of the jet

The jet dispersion characteristics in air along the radial direction are shown in Figs. 9 and 10. Fig. 9 shows the effect of the standoff distance on the jet dispersion when the abrasive particle size is 0.18 mm. In Fig. 9(a), a radial position (r) of zero indicates the central axis of the jet, where the velocity reaches its maximum value for each standoff distance. The maximum velocity along the central axis decreased as the standoff distance increased. This is because a drag force is applied to the abrasive particles owing to the air resistance. Additionally, the radial position

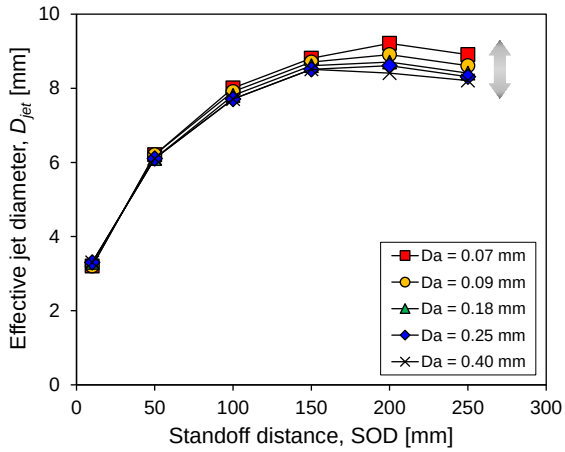

Fig. 12 Effective jet diameter depending on the standoff distance

with the same abrasive velocity increases with the standoff distance, indicating greater jet dispersion in air as the distance between the AWJ system and the rock material increases. In terms of the abrasive kinetic energy, Fig. 9(b) shows that the jet is relatively more dispersed as the standoff distance increases. Therefore, the drilling width is expected to increase with the standoff distance when rocks are drilled using an AWJ.

Fig. 10 shows the effect of abrasive particle size on jet dispersion at a standoff distance of 100 mm. As can be seen in Fig. 10(a), the effect of abrasive particle size on abrasive velocity was minimal. The abrasive velocity at the center axis where the radial position is zero showed a relatively different effect depending on the abrasive particle size, but showed a similar distribution across the radial positions. On the other hand, the effect of abrasive particle size on abrasive kinetic energy was significant (Fig. 10(b)). While the difference in the abrasive velocity was not large, variations in abrasive kinetic energy arose owing to the differences in particle mass associated with the abrasive particle size. When comparing the abrasive kinetic energies at the same radial position, relatively larger energy was distributed as the abrasive particle size increased. This can lead to an increase in the drilling width of the AWJ. Therefore, it is predicted that, when rock is drilled using an AWJ, the drilling width increases with the abrasive particle size. However, accurate prediction of the drilling performance required additional consideration of the number of abrasive particles at each radial position.

4.3 Effective jet diameter

4.3.1 Influence of the standoff distance

To define the effective jet diameter (D_{jet}), the critical jet radius (R_c) must be determined, and the number of abrasive particles (N_a) and the total abrasive kinetic energy ($E_{a,t}$) must first be understood. Fig. 11 shows the effect of standoff distance on the number and total energy of the abrasive particles when the abrasive particle size was 0.40 mm. Fig. 11(a) shows the number of abrasive particles calculated using Eq. (6), which shows different results

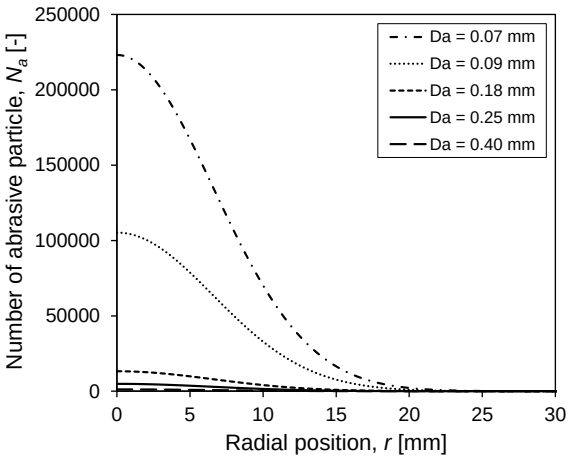

(a) Number of abrasive particles

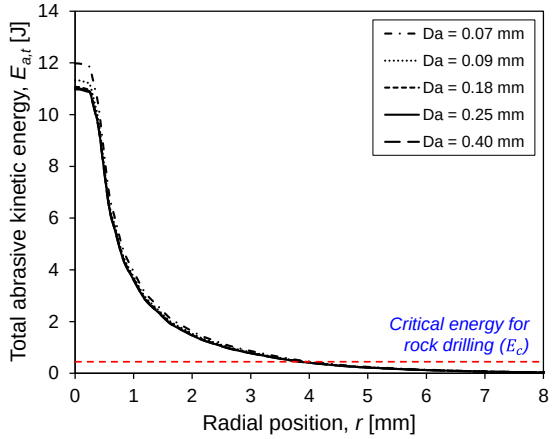

(b) Total kinetic energy of abrasive particles

Fig. 13 Effect of the abrasive particle size on the number and total kinetic energy of the abrasive particle (standoff distance of 150 mm)

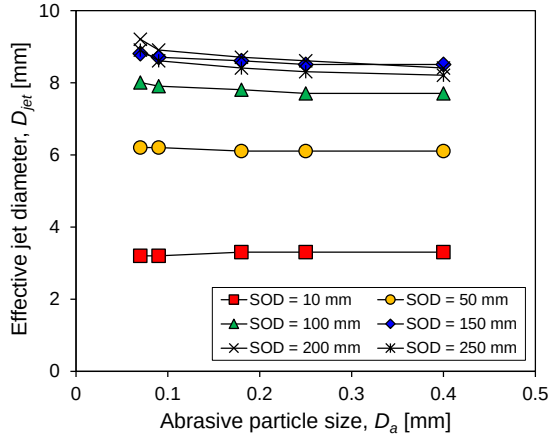

Fig. 14 Effective jet diameter depending on the abrasive particle size

depending on the standoff distance. As the standoff distance decreases, the number of abrasive particles at the central axis of the jet increases, and the abrasive particles are primarily distributed near the central axis. However, as the standoff distance increased, the absolute number of abrasive particles at the central axis of the jet decreased, and the particles were widely distributed radially from the central axis.

Fig. 11(b) shows the results of the total abrasive kinetic energy ($E_{a,t}$) calculated using Eq. (7), where the number of abrasive particles and kinetic energy of the abrasive particles are comprehensively considered. As this is the total energy per radial position received by the rock during drilling, it can be assumed to correspond to the shape of the hole drilled by the AWJ. As the standoff distance increases, the drilling depth is expected to decrease, while the drilling width increases.

Fig. 12 shows the effective jet diameter (D_{jet}) calculated using Eq. (9). This was calculated by deriving the critical jet radius (R_c) based on the critical energy for rock drilling (E_c) of 0.36 J determined in Section 4.1, as shown in Fig. 11. The effective jet diameter (D_{jet}) increased with standoff distance and then decreased, indicating an optimal standoff distance. The optimal standoff distance is influenced by multiple system parameters, including water pump pressure, and water flow rate, as these factors directly affect the jet's kinetic energy and dispersion characteristics. However, in this study, the water pump pressure and water flow rate were kept constant across all simulation cases to systematically analyze the effective jet diameter (D_{jet}) as a function of standoff distance.

Under these controlled conditions, the optimal standoff distance, defined in terms of maximizing the effective jet diameter, was found to be approximately 150–200 mm, varying somewhat depending on the abrasive particle size. In addition, it was determined that the effective jet diameter (D_{jet}) was significantly affected by the abrasive particle size as the standoff distance increased. Therefore, to evaluate and predict the effective jet diameter accurately, a comprehensive consideration of the standoff distance and abrasive particle size is necessary.

4.3.2 Influence of the abrasive particle size

Fig. 13 shows the effect of the abrasive particle size on the number and total energy of the abrasive particles when the standoff distance was 150 mm. Fig. 13(a) shows the number of abrasive particles calculated using Eq. (6), indicating a large difference depending on the abrasive particle size. Because this numerical analysis was performed under the condition of inputting the same abrasive flow rate (i.e., 5 g/s), the number of abrasive particle inputs increased as the abrasive particle size decreased. Therefore, the number of abrasive particles at the central axis of the jet differed significantly, depending on the abrasive particle size. However, as mentioned in Section 4.2.2, because the abrasive kinetic energy of a single abrasive particle differs depending on the abrasive particle size, it is necessary to comprehensively analyze the total abrasive kinetic energy. Fig. 13(b) shows the results of the total abrasive kinetic energy ($E_{a,t}$) calculated using Eq. (7), which can be assumed to be the shape of the drilled hole in terms of the total energy received by the rock per radial position. As the abrasive particle size increases, the total abrasive kinetic energy at the central axis of the jet

decreases, whereas the effect in the radial direction is minimal. Therefore, it is predicted that the rock drilling performance of the AWJ will decrease as the abrasive particle size increases, whereas the drilling width will remain constant.

Fig. 14 shows the effective jet diameter (D_{jet}) calculated using Eq. (9) and the effect of the abrasive particle size. The impact of the abrasive particle size on the effective jet diameter (D_{jet}) was found to be insignificant. As the abrasive particle size increased, the effective jet diameter (D_{jet}) remained constant. However, the degree of the effect of the abrasive particle size on the effective jet diameter (D_{jet}) varied depending on the standoff distance. When the standoff distance was 150 mm or more, the effective jet diameter (D_{jet}) decreased as the abrasive particle size increased. It was found that the larger the standoff distance, the greater the effect of the abrasive particle size on the effective jet diameter, and under conditions where the standoff distance is large, it is efficient in terms of the effective jet diameter to use abrasive particles with relatively small sizes. Therefore, when drilling rocks using an AWJ in the field, selecting an appropriate abrasive particle size according to various standoff distance environments is crucial to achieving effective drilling performance.

5. Conclusions

This study analyzed the jet flow characteristics in air by numerical analysis, considering various standoff distances and abrasive particle sizes. The jet flow characteristics were observed in the axial and radial directions and evaluated by analyzing the abrasive particle velocity and kinetic energy, respectively. In addition, the critical energy for rock drilling was derived and an effective jet diameter considering the number of abrasive particles at each position was proposed. Based on this, the expected drilling performance of the AWJ in rock drilling was evaluated. In particular, the possibility of optimizing the rock drilling efficiency of the AWJ by appropriately combining the standoff distance and abrasive particle size is suggested. In addition, this study demonstrates that the jet flow behavior in air, which is challenging to observe experimentally, can be quantitatively predicted using a numerical analysis approach. The study results are expected to provide fundamental data for system design and abrasive selection strategies for effectively applying the AWJ technology to geotechnical and mining fields. The main findings of this study are as follows.

• Based on the minimum critical pressure of AWJ for hard rock from a previous study, the critical energy for rock drilling (E_c) was estimated to be approximately 0.36 J through CFD simulation.

• The abrasive velocity and kinetic energy of the axial jet decreased as the standoff distance increased, owing to the energy loss caused by air resistance. As the abrasive particle size increases, the abrasive velocity decreases, but the abrasive kinetic energy increases.

• As the standoff distance increased, the abrasive velocity and kinetic energy of the radial jet flow became more widely distributed owing to greater loss of straightness from air resistance. While the abrasive velocity exhibited little change with increasing abrasive particle size, the abrasive kinetic energy increased. This suggests that the abrasive kinetic energy is more dependent on the abrasive particle mass than on abrasive velocity.

• The effective jet diameter (D_{jet}) is affected by the standoff distance and abrasive particle size, and an optimal combination exists. As the standoff distance increased, the effective jet diameter first increased and then decreased. In particular, when the standoff distance was greater than 100 mm, the abrasive particle size significantly affected the effective jet diameter. Therefore, to perform efficient rock drilling, it is necessary to design an appropriate standoff distance and abrasive particle size according to field conditions.

The findings of this study provide valuable insights into optimizing abrasive waterjet (AWJ) drilling performance in geotechnical and mining applications. The results demonstrate that the effective jet diameter (D_{jet}) is significantly influenced by standoff distance and abrasive particle size, highlighting the importance of selecting appropriate operating conditions. In practical applications, the identification of an optimal standoff distance of approximately 150–200 mm provides a useful guideline for determining nozzle positioning, while the influence of abrasive particle size suggests that adjusting its selection based on field conditions can improve drilling efficiency.

Additionally, the study offers a quantitative understanding of jet energy distribution, which can aid in optimizing AWJ system parameters to enhance energy efficiency and reduce abrasive consumption. By carefully selecting drilling parameters, practitioners can minimize energy waste while improving operational performance. These insights are expected to be valuable for engineers working with AWJ systems, particularly in rock drilling and material removal. Future research could further refine these findings by considering variable water pump pressure and water flow rate conditions to expand the applicability of the proposed approach.

Acknowledgments

This work was supported by a grant (RS-2023-00245334) funded by Korea of Ministry of Land, Infrastructure and Transport (MOLIT) and with technical support from ANSYS Korea. The third author was supported by the Innovated Talent Education Program for Smart City from MOLIT.

References

Alberdi, A., Rivero, A., López de Lacalle, L.N., Etxeberria, I. and Suárez, A. (2010), "Effect of process parameter on the kerf geometry in abrasive water jet milling", *Int. J. Adv. Manuf. Technol.*, **51**, 467-480. https://doi.org/10.1007/s00170-010-2662-y.

Balz, R. and Heiniger, K.C. (2011), "Determination of spatial velocity distributions of abrasive particles in abrasive water jets using laser-induced fluorescence under real conditions",

Proceedings of the 16th WJTA-IMCA Conference and Expo, September.

Cha, Y., Oh, T.M., Joo, G.W. and Cho, G.C. (2021), "Performance and reuse of steel shot in abrasive waterjet cutting of granite", *Rock Mech. Rock Eng.*, **54**, 1551-1563. https://doi.org/10.1007/s00603-020-02332-8.

Evans, A.G., Gulden, M.E. and Rosenblatt, M. (1978), "Impact damage in brittle materials in the elastic-plastic response regime", *Proceedings of the Royal Society of London. A. Mathematical and Physical Sciences*, **361**(1706), 343-365. https://doi.org/10.1098/rspa.1978.0106.

Fluent ANSYS (2023), ANSYS Fluent 2023 R2 User's Guide And Theory Manual. ANSYS Inc., USA.

Forder, A., Thew, M. and Harrison, D. (1998), "A numerical investigation of solid particle erosion experienced within oilfield control valves", *Wear*, **216**(2), 184-193. https://doi.org/10.1016/S0043-1648(97)00217-2.

Gong, Q., Yin, L., Ma, H. and Zhao, J. (2016), "TBM tunnelling under adverse geological conditions: an overview", *Tunn. Undergr. Sp. Tech.*, **57**, 4-17. https://doi.org/10.1016/j.tust.2016.04.002.

Hashish, M. (1991), "Characteristics of surfaces machined with abrasive-waterjets", *J. Eng. Mater. Technol*., **113**, 354-362. https://doi.org/10.1115/1.2903418.

Horszczaruk, E.K. (2009), "Hydro-abrasive erosion of high performance fiber-reinforced concrete", *Wear*, **267**(1-4), 110-115. https://doi.org/10.1016/j.wear.2008.11.010.

Hou, R.G., Huang, C.Z., Zhu, H.T. and Niu, Z.W. (2010), "The measurement of the velocity outside the high pressure water jet and abrasive water jet nozzle based on the energy transfer method", *Adv. Mater. Res.*, **135**, 361-364. https://doi.org/10.4028/www.scientific.net/AMR.135.361.

Hwang, B., Choi, H., Kwon, K., Shin, Y.J. and Kang, M. (2024a), "Prediction models of rock quality designation during TBM tunnel construction using machine learning algorithms", *Geomech. Eng.*, **38**(5), 507-515. https://doi.org/10.12989/gae.2024.38.5.507.

Hwang, H.J., Cha, Y., Kang, S.J. and Cho, G.C. (2024b), "Semi-empirical model for abrasive particle velocity prediction in abrasive waterjet based on momentum transfer efficiency", *Comput. Part. Mech.*, 1-13. https://doi.org/10.1007/s40571-024-00747-6.

Isobe, T. (1988), "Distribution of abrasive particles in abrasive water jet and acceleration mechanism", *Proceedings of the 9th International Symposium on Jet Cutting Technology*, (Vol. 217).

Jafar, R.H.M., Nouraei, H., Emamifar, M., Papini, M. and Spelt, J.K. (2015), "Erosion modeling in abrasive slurry jet micro-machining of brittle materials", *J. Manuf. Proc.*, **17**, 127-140. https://doi.org/10.1016/j.jmapro.2014.08.006.

Karakurt, I., Aydin, G. and Aydiner, K. (2012), "A study on the prediction of kerf angle in abrasive waterjet machining of rocks", *Proc. Inst. Mech. Eng. B J. Eng. Manuf.,* **226**(9), 1489-1499.

Karakurt, I., Aydin, G. and Aydiner, K. (2014), "An investigation on the kerf width in abrasive waterjet cutting of granitic rocks", *Arab. J. Geosci.*, **7**, 2923-2932. https://doi.org/10.1007/s12517-013-0984-4.

Launder, B.E. and Spalding, D.B. (1983), "The numerical computation of turbulent flows", *Numerical prediction of flow, heat transfer, turbulence and combustion,* 96-116, Pergamon press. https://doi.org/10.1016/B978-0-08-030937-8.50016-7.

Lee, G.J., Ryu, H.H., Cho, G.C. and Kwon, T.H. (2023), "Full-scale TBM excavation tests for rock-like materials with different uniaxial compressive strength", *Geomech. Eng.*, **35**(5), 487-497. https://doi.org/10.12989/gae.2023.35.5.487.

Li, H., Liu, S., Zhou, F., Jiang, H., Wang, F. and Guo, C. (2022), "Experimental investigation on concrete rock breaking performance of self-excited oscillation pulsed waterjet", *Eng. Fract. Mech.*, **268**, 108502. https://doi.org/10.1016/j.engfracmech.2022.108502.

Liu, H., Wang, J., Brown, R.J. and Kelson, N. (2003), "Computational fluid dynamic (CFD) simulation of ultrahigh velocity abrasive waterjet", *Key Eng. Mater.*, **233-236**, 477-482.

Liu, H., Wang, J., Kelson, N. and Brown, R.J. (2004), "A study of abrasive waterjet characteristics by CFD simulation", *J. Mater. Process Technol.*, **153**, 488-493. https://doi.org/10.1016/j.jmatprotec.2004.04.037.

Liu, Q., Huang, X., Gong, Q., Du, L., Pan, Y. and Liu, J. (2016), "Application and development of hard rock TBM and its prospect in China", *Tunn. Undergr. Sp. Tech.*, **57**, 33-46. https://doi.org/10.1016/j.tust.2016.01.034.

Liu, Z.H., Du, C.L., Zheng, Y.L., Zhang, Q.B. and Zhao, J. (2017), "Effects of nozzle position and waterjet pressure on rock-breaking performance of roadheader", *Tunn. Undergr. Sp. Tech.*, **69**, 18-27. https://doi.org/10.1016/j.tust.2017.06.003.

Lu, Y., Tang, J., Ge, Z., Xia, B. and Liu, Y. (2013), "Hard rock drilling technique with abrasive water jet assistance", *Int. J. Rock Mech. Mining Sci.*, **60**, 47-56. https://doi.org/10.1016/j.ijrmms.2012.12.021.

Lv, Z., Hou, R., Tian, Y., Huang, C. and Zhu, H. (2018), "Investigation on flow field of ultrasonic-assisted abrasive waterjet using CFD with discrete phase model", *Int. J. Adv. Manuf. Technol.*, **96**, 963-972. https://doi.org/10.1007/s00170-018-1635-4.

Momber, A.W. (2004), "Wear of rocks by water flow", *Int. J. Rock Mech. Mining Sci.*, **41**(1), 51-68. https://doi.org/10.1016/S1365-1609(03)00075-3.

Momber, A. (2011), *Hydrodemolition Of Concrete Surfaces And Reinforced Concrete*, Elsevier Science,

Momber, A.W. and Kovacevic, R. (1995), "Energy dissipative processes in high speed water-solid particle erosion", *ASME-Publications-Htd*, **321**, 555-564.

Momber, A.W. and Kovacevic, R. (2012), *Principles Of Abrasive Water Jet Machining*, Springer Science & Business Media.

Nagaraja, D.K.T. and Devadula, S. (2023), "A generic model for prediction of kerf cross-sectional profile in multipass abrasive waterjet milling at macroscopic scale by considering the jet flow dynamics", *Int. J. Adv. Manuf. Technol.*, **127**(5), 2815-2841. https://doi.org/10.1007/s00170-023-11683-9.

Nambiath, P., Galecki, G. and Summers, D.A. (2007). Energy based modelling of abrasive slurry jet", *Proceeding of the 2007 American Water Jet Conference,* Texas*,* August.

Oh, T.M. and Cho, G.C. (2014), "Characterization of effective parameters in abrasive waterjet rock cutting", *Rock Mech. Rock Eng.*, **47**, 745-756. https://doi.org/10.1007/s00603-013-0434-3.

Oh, T.M. and Cho, G.C. (2016), "Rock cutting depth model based on kinetic energy of abrasive waterjet", *Rock Mech. Rock Eng.*, **49**, 1059-1072. https://doi.org/10.1007/s00603-015-0778-y.

Roth, P., Looser, H., Heiniger, K.C. and Bühler, S. (2005), "Determination of abrasive particle velocity using laser-induced fluorescence and particle tracking methods in abrasive water jets", *Proceedings of the 2005 WJTA Conference and Exposition,* August.

Samadi, H., Hassanpour, J. and Rostami, J. (2023), "Prediction of earth pressure balance for EPB-TBM using machine learning algorithms", *Int. J. Geo-Eng.*, **14**(1), 21. https://doi.org/10.1186/s40703-023-00198-7.

Samadi, H., Hassanpour, J. and Rostami, J. (2024), "Assessment of shear strength of fine-grained and coarse-grained soil using actual EPB-TBM operating data", *Int. J. Geo-Eng.,* **15**(1), 20. https://doi.org/10.1186/s40703-024-00220-6.

She, L., Li, Y.L., Wang, C., Zhang, S.R., He, S.W., Liu, W.J. and Li, S.M. (2023), "Prediction of TBM disc cutter wear based on field parameters regression analysis", *Geomech. Eng.*, **35**(6),

647-663. https://doi.org/10.12989/gae.2023.35.6.647.
Streeter, V.L. and WE, B.K. (1998). Fluid mechanics. WCB McGraw-Hill. Inc. Boston.
Summers, D.A. (2003), "Waterjetting technology", CRC Press.
Thongkaew, K. and Wang, J. (2017), "An experimental study of the particle velocities in abrasive waterjets", *Int. J. Abrasive Technol.*, **8**(2), 147-156. https://doi.org/10.1504/IJAT.2017.089291.
Wang, R. and Wang, M. (2010), "A two-fluid model of abrasive water jet", *J. Mater. Process. Technol.*, **210**(1), 190-196. https://doi.org/10.1016/j.jmatprotec.2009.06.007.
Yanaida, K. and Ohashi, A. (1974), "Flow characteristics of water jets", *Proceedings of the 2nd International Symposium on Jet Cutting Technology*, April.
Zeleňák, M., Foldyna, J., Linde, M., Pude, F., Rentsch, T., Fernolendt, J. and Poort, H.U. (2016), "Measurement and analysis of abrasive particles velocities", *Procedia Eng.*, **149**, 77-86. https://doi.org/10.1016/j.proeng.2016.06.641.
Zhang, J., Li, Y., Zhang, Y., Yang, F., Liang, C. and Tan, S. (2020), "Using a high-pressure water jet-assisted tunnel boring machine to break rock", *Adv. Mech. Eng.*, **12**(10), 1687814020962290. https://doi.org/10.1177/1687814020962290.
Zou, X., Fu, L. and Wu, L. (2024) "Multiphase flow and nozzle wear with CFD-DEM in high-pressure abrasive water jet", *Powder Technol.*, **444**, 120019. https://doi.org/10.1016/j.powtec.2024.120019.